Low-field vortex patterns in the multiband $BaFe_{2-x}Ni_xAs_2$ superconductor (x = 0.1, 0.16)

L. J. Li,[1,*] T. Nishio,[2] Z. A. Xu,[3] and V. V. Moshchalkov[1,†]

[1]*INPAC—Institute for Nanoscale Physics and Chemistry, KULeuven, Celestijnenlaan 200D, Leuven 3001, Belgium*

[2]*Department of Physics, Tokyo University of Science, Shinjuku, Tokyo 162-8601, Japan*

[3]*Physics Department, Zhejiang University, Hangzhou 310027, China*

(Received 4 December 2010; revised manuscript received 28 April 2011; published 29 June 2011)

The distribution of vortices at low magnetic fields in single crystals of multiband $BaFe_{2-x}Ni_xAs_2$ (x = 0.1 and x = 0.16) superconductors is studied by Bitter decoration. Highly inhomogeneous vortex patterns, including vortex stripes and vortex clusters, are observed. The origin of these inhomogeneous vortex arrays is likely to be due to strong flux pinning, as suggested by magnetization measurements performed at high fields. Alternative possible scenarios, such as type-1.5 superconductivity due to multiband effect, are also discussed.

DOI: 10.1103/PhysRevB.83.224522 PACS number(s): 74.25.Ha, 74.25.Uv, 74.25.Sv, 74.25.Wx

I. INTRODUCTION

The arrangements of vortices in type-II superconductors are very closely linked to fundamental properties of the superconducting state. For instance, the triangular Abrikosov lattice can be transformed into a lower symmetry lattice reflecting the shape of the Fermi surface,[1,2] the symmetry of the superconducting gap,[3] or the crystal anisotropy.[4] Arguably one of the most sensitive parameters determining the vortex distribution is the pinning landscape where small variations in the material properties (such as critical temperature, mean free path, off-stoichiometry, etc.) may cause profound distortions to the ideal lattice. Thus, vortices can agglomerate to form clusters of individual flux quantum units nearby pinning centers, can even coalesce into giant vortices for relatively large pinning sites, or form patterns reproducing the underlying pinning landscape such as correlated planar defects or artificial pinning centers.

Interestingly, it has been shown that even in the complete absence of pinning, unusual vortex structures such as clusters and stripes can also emerge from competing vortex-vortex interactions, i.e., when the interaction does not have a monotonous dependence on the intervortex distance. This is, for example, the case for vortices in an anisotropic superconductor tilted away from the principal symmetry axes, where an attractive interaction results from the change of sign of the component parallel to the vortex direction of the field generated by a vortex line.[5] A similar field reversal in the magnetic field distribution of an isolated vortex results from the nonlocal relationship between supercurrents and vector potential in clean low-k materials.[6] It has been shown that this effect also leads to an attractive vortex-vortex interaction. Yet another example has been recently proposed[7] for the case of two-component superconductors where two weakly coupled order parameters, each of which belong to a different type of superconductivity, coexisting in the same material, which is coined as type-1.5 superconductivity (type-1.5 SC).[8–10]

The fact that particular static pinning landscapes or the interplay of competing long-range attractive and short-range repulsive vortex-vortex interaction can both lead to vortex clustering makes it difficult to conclude, based solely on vortex images, which of the two scenarios is applicable or whether both phenomena are present simultaneously.

In this work we focus on the vortex pattern formation in the recently discovered iron-pnictide materials where vortex clustering is clearly visible in a broad range of magnetic fields. We show that unusual vortex distributions appear in optimally doped and overdoped $BaFe_{2-x}Ni_xAs_2$ ($BaNi_x$) (x = 0.1 and x = 0.16, respectively) single crystals at low applied fields ($H_a \leqslant 10$ Oe). We found that the distribution of vortices is highly inhomogeneous in both samples, at any field within the explored field range. The most striking observations are the stripe-like vortex patterns, similar to those observed in MgB_2. However, through magnetization measurements we infer that these samples lie in the strong pinning limit, unlike MgB_2 studied in Ref. 8. We discuss the possible mechanisms of the stripe-like vortex patterns in terms of different sources of pinning and contrast it with the scenario of unconventional vortex-vortex interaction arising from multiband effects. This report broadens considerably previous studies of the vortex lattice patterns in pnictide superconductors mainly conducted on 122 series $Ba_{1-x}K_xFe_2As_2$ or $BaFe_{2-x}Co_xAs_2$ single crystals by decoration,[11] neutron diffraction,[12] scanning tunneling microscopy,[13] and magnetic force microscopy.[14]

II. EXPERIMENTAL

Single crystals of $BaNi_x$ (nominally x = 0.1 and x = 0.16) superconductors were grown by a self-flux method as described elsewhere.[15] Similar samples from the same group have been previously used in other experiments.[16–18] The chemical compositions of the samples were confirmed by energy-dispersive x-ray spectrometry (EDX).[19] The onset of the superconducting transition temperature is 20.5 K for x = 0.1 and 11.5 K for x = 0.16, with transition widths below 1.0 K as determined from magnetic susceptibility measured at 10 Oe in a commercial Physical Properties Measurement System (PPMS-6000) by Quantum Design. Field-dependent magnetization measurements were carried out in Magnetic Properties Measurement System (MPMS-XL) by Quantum Design with maximum field up to 6 T. For Bitter decoration experiments, crystals were freshly cleaved along the planes, which are perpendicular to the *c*-axis to acquire shiny and clean surfaces. The samples were then cooled down to 4.2 K with a magnetic field applied perpendicular to the cleaved surfaces. Iron particles were evaporated within a few seconds and

deposited onto the sample surface under a suitable pressure of a helium atmosphere. An approximate 2 K temperature gradient may be present during the evaporation. The $NbSe_2$ single crystals with $T_c = 7.2$ K and transition width <0.1 K were always used as reference samples to control the quality of the decoration. To visualize the locations of iron particle islands that indicate the positions of the vortices, scanning electron microscopy (SEM-JSM-5600) was used. In the investigation of the vortex structure in the same sample at different magnetic fields, the previously decorated thin surface layer was removed by cleaving it with adhesive scotch tape, thus, exposing a new clean surface of the crystal, which can be reused.

III. RESULTS AND DISCUSSION

For all investigated fields, $H_a \leqslant 10$ Oe, the positions of the superconducting vortices in $NbSe_2$ single crystals are well resolved. Due to the low pinning and type-II behavior, slightly distorted triangular lattices are mainly observed in $NbSe_2$ single crystals. In contrast to that, the vortices are not always clearly resolved in $BaNi_x$ single crystals, which is possibly due to the larger penetration depth of the iron-pnictide superconductors (~300 nm)[14] and the degradable surface quality because of oxidization. Furthermore, we observed no triangular lattices but very inhomogeneous vortex distribution in $BaFe_{2-x}Ni_xAs_2$ single crystals in all the explored fields.

A. Optimally doped $BaNi_{0.1}$

Figure 1 shows typical Bitter decoration images at $H_a = 1$ Oe obtained on (a) $BaNi_{0.1}$ and (b) $NbSe_2$ single crystals decorated simultaneously. Contrary to the conventional homogeneous triangular vortex pattern in $NbSe_2$, a very inhomogeneous vortex distribution is observed on $BaNi_{0.1}$ single crystal, somewhat similar to the vortex pattern observed previously in MgB_2.[8] A Delaunay-triangulation (i.e., lines connecting first neighbors) of the vortex structure is shown in Figs. 1(c) and 1(d). The vertices of each triangle represent the locations of the vortices. From these plots, it is easy to identify the vortex-sparse areas like those marked in light gray and the vortex-dense areas marked in dark gray in $BaNi_{0.1}$ in contrast to the uniform vortex distribution in $NbSe_2$. Through the triangulation, we calculated the distribution of first-neighbor distance of vortices, P_a [displayed in Figs. 1(e) and 1(f)] in order to characterize the inhomogeneity of the vortex patterns. As one can see, the vortex distribution in $NbSe_2$ follows a Gaussian form with a standard deviation of 2 μm similar to the value obtained in a previous report.[8] In contrast to that, the vortex distribution in $BaNi_{0.1}$ is considerably broader with a standard deviation of 3.6 μm.

Figure 2 shows the vortex patterns of $BaNi_{0.1}$ at $H_a = 5$ Oe. We found that at this field, two different types of vortex patterns develop. In most areas of the sample [shown in Fig. 2(a)], vortices agglomerate to form clusters, which are separated by vortex voids, whereas in some smaller regions of the sample [shown in Fig. 2(b)], vortex chains and vortex voids are formed similarly to the stripe-like vortex patterns observed in MgB_2. However, through the data collected from several pieces of the decorated sample, we estimate that these regions with stripe-like vortex patterns occupy approximately 5% of the whole decorated sample surface and are distributed randomly. Figure 2(c) shows a zoom-in of the area enclosed by the dashed line in Fig. 2(b).

At a higher field $H_a = 10$ Oe, the vortex distribution remains highly inhomogeneous, as shown in Fig. 3, which is consistent with previous reports.[11] This is in contrast to the case of MgB_2, which at $H_a \geqslant 10$ Oe, the homogeneous vortex patterns are recovered corresponding to a regular Abrikosov lattice.[8] At this field, we still observe the two characteristic vortex patterns, clusters and stripes, very much like the patterns observed at $H_a = 5$ Oe. The fraction of the areas taken by those stripe-like vortex patterns remains ~5%. However, we cannot confirm that the stripe-like patterns are in the same positions as those observed in $H_a = 5$ Oe only by Bitter decoration. Compared to the direct visualizing techniques, such as Hall probe, magnetic force microscopy, etc., Bitter decoration is not an *in situ* technique. Due to the different topography of the sample surface after each cleaving, it is nearly impossible to locate exactly the same position of the sample surface in SEM in two different decorations.

In order to reveal whether the observed flux distribution is caused by a highly inhomogeneous pinning landscape, we measured magnetization hysteresis loops on a crystal with dimensions of $3.35 \times 1.5 \times 0.25$ mm^3 with the field applied along the c-axis. Figure 4(a) summarizes these measurements carried out for several temperatures. Here, a second magnetization peak is clearly visible. The observation of this second peak, which is rather broad, was also reported in previous publications.[20–22] This peak is usually considered to be a sign of the transition between the elastic and the plastic vortex pinning regimes. Based on the Bean critical state model,[23] the critical current density can be estimated from the width, ΔM, of the magnetization loops, by using the equation,

$$J_c = 20\Delta M/w(1 - w/3l),$$

where w and l are the width and the length of the sample, respectively. The resulting critical current density versus field is plotted in Fig. 4(b). The critical current J_c at 4.2 K and low fields (close to the conditions used for decoration) is as high as 4×10^5 A/cm^2 and after a sharp decrease at low fields, it remains nearly field independent only following the smooth modulation due to the presence of a broad second magnetization peak. By plotting J_c as a function of reduced temperature T/T_c for different applied fields [see Fig. 4(b)], a clear scaling can be seen at low temperatures. This is an indication that the same pinning regime persists for all these fields. This allows us to link the two experimental methods: Bitter decorations at low fields and magnetizations measurements at high fields.

B. overdoped $BaNi_{0.16}$

Bitter decoration experiments show that the vortex distribution in $BaNi_{0.16}$ single crystals at all investigated fields is also inhomogeneous. The main differences with the results obtained for the optimally doped sample appear in the vortex patterns at $H_a = 5$ Oe and 10 Oe (see Fig. 5). Although vortices still form disordered clusters and chains, similar to the patterns from most regions of the optimally doped sample, we can find stripe-like vortex patterns only in relatively small randomly distributed areas, which are marked by the solid white frames

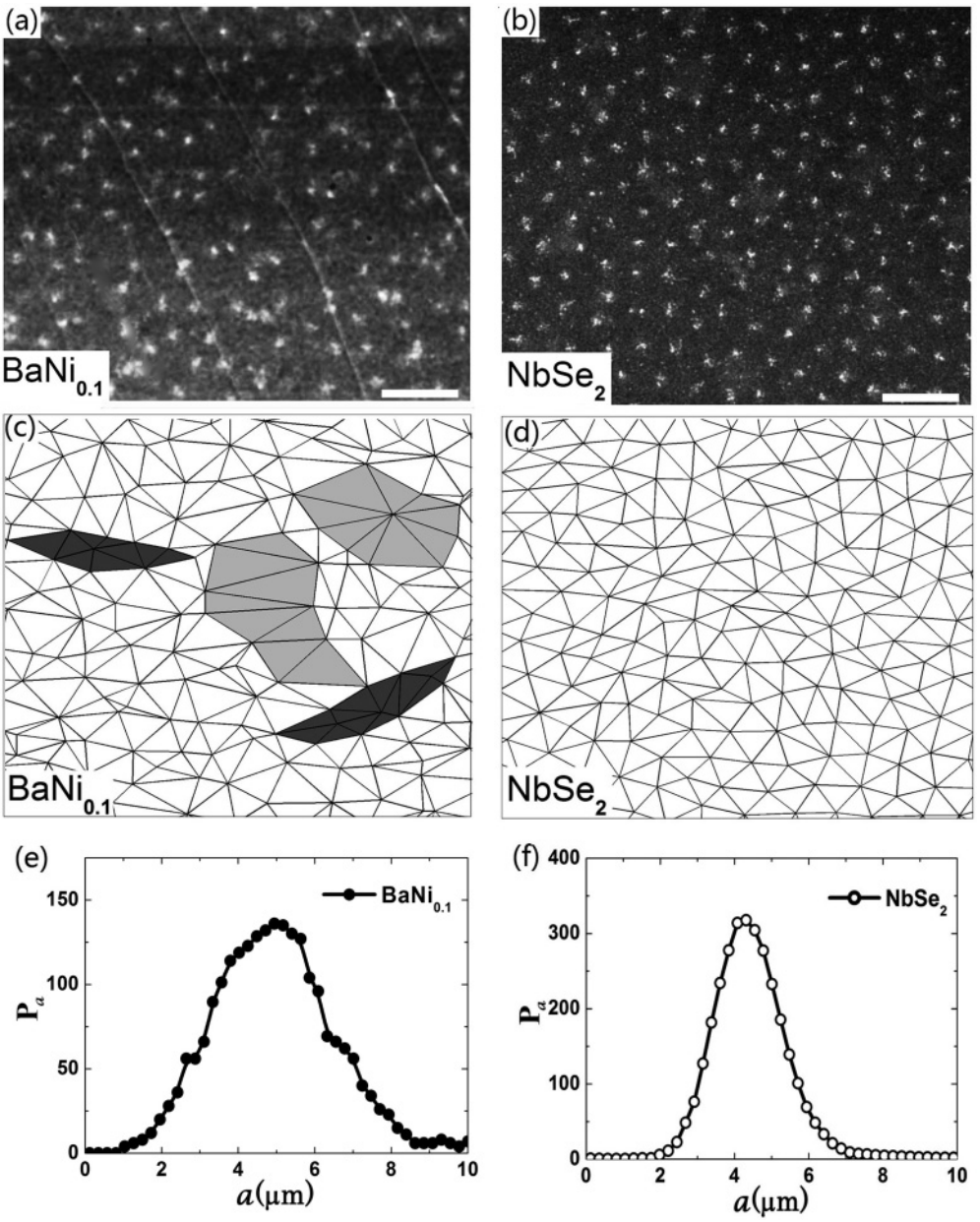

FIG. 1. Bitter decoration images at $H_a = 1$ Oe of (a) $BaNi_{0.1}$, (b) $NbSe_2$. The scale bars in the images correspond to 10 μm. Panels (c) and (d) show Delaunay triangulation: vertices of the triangle indicate the position of the vortices. Light-gray and dark-gray areas represent the vortex-sparse and vortex-dense areas, respectively. Panels (e) and (f) show the distribution of first-neighbor distance of vortices, P_a.

in Fig. 5. The percentage of the area taken by these stripe-like vortex patterns is difficult to evaluate, because the stripes can be a very small size in some areas, and challenging to clearly identify. Complementary information on the pinning strength in $BaNi_{0.16}$ single crystals has been obtained by carrying out magnetization measurements (the dimensions of the crystal: $2.25 \times 1.2 \times 0.2$ mm^3), as displayed in Fig. 6. Compared with the optimally doped sample, the smaller J_c values and their faster decrease with both increasing field and temperature demonstrate that the pinning in the overdoped sample is weaker. It is worth noting that this reduction in the critical current does not arise from the drop in T_c. Indeed, the critical transition temperature of the overdoped sample is about half of that of the optimally doped sample, at $T = 0.2T_c$, the critical current value of the overdoped sample is only one-fifth of the optimally doped sample. The weaker pinning in the overdoped sample has also been seen in a previous report.[20] Nevertheless, compared with MgB_2 single crystals, in which the weak bulk pinning is indicated by the dominant reversible magnetization,[24] the pinning strength in $BaNi_x$ single crystals is considerably stronger.

There are several possibilities to explain the vortex clusters and vortex stripes we have observed in $BaNi_x$ single crystals. First, within the strong pinning scenario, the possible correlated pinning sites can be caused by twin boundaries or induced by local fluctuations of the doping concentration.

Naturally, the parallel stripes and their almost 90° crossing in optimally doped samples resemble the effect of the twin

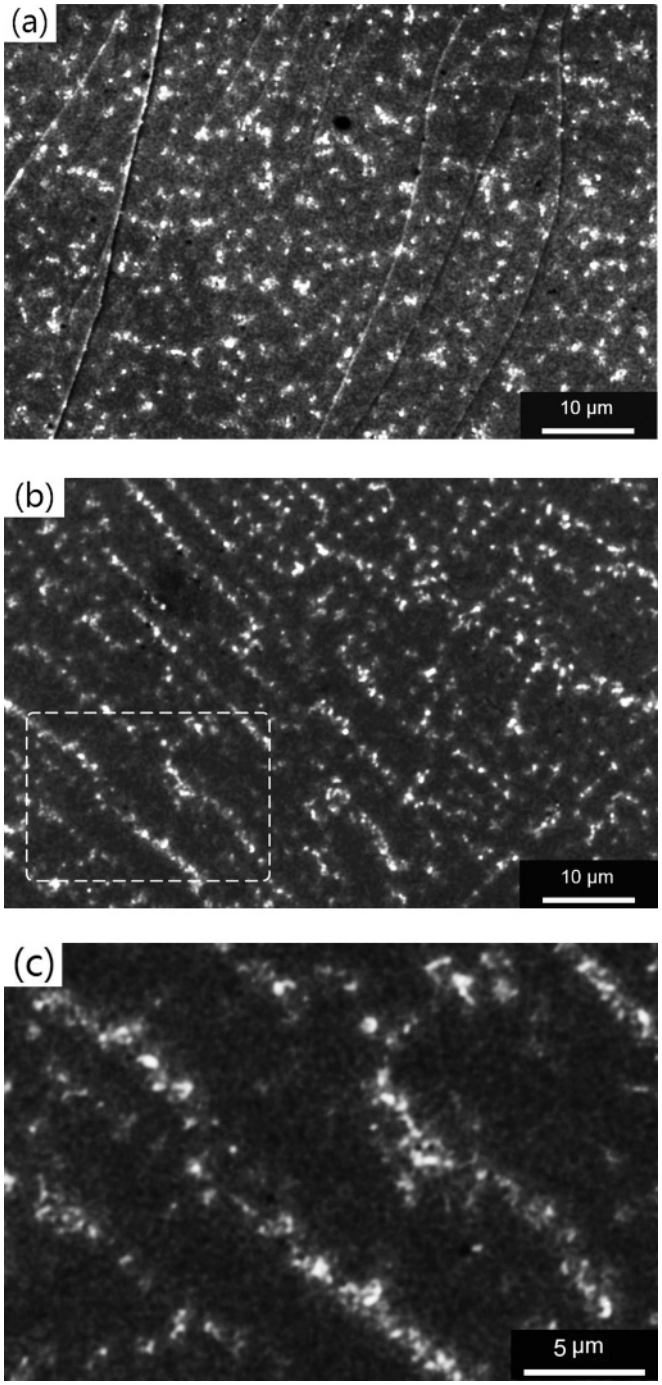

FIG. 2. Images of representative vortex structure obtained by Bitter decoration at $H_a = 5$ Oe of $BaNi_{0.1}$ single crystals. (a) Most regions of the sample exhibit clustering of vortices. (b) About 5% of the total area of the sample shows stripe patterns. (c) Zoom-in of the area enclosed by the dashed line in (b).

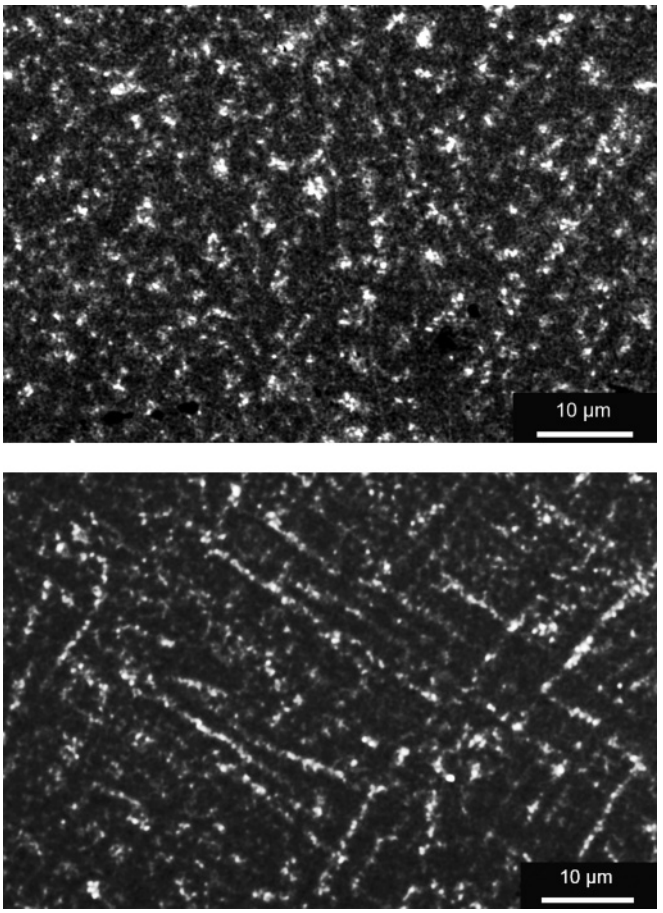

FIG. 3. Typical Bitter decoration vortex pattern derived for $BaNi_{0.1}$ single crystals at $H_a = 10$ Oe. Upper image: from most regions of the sample; lower image: from some small regions of the sample.

boundaries. Twin boundaries are known as one type of the correlated pinning centers in cuprates[25,26] and RNi_2B_2C[27,28] (R = Er, Ho) layered compounds. It is also reported that twin boundaries exist in undoped and underdoped pnictide single crystals[29] but are absent in optimally doped and overdoped samples.[30] However, as reported by Prozorov *et al.*,[31] a maze of fine intersecting domain boundaries can appear in the sample from underdoped up to an almost optimal doping level and could eventually lead to a substantial intrinsic pinning. Those interwoven structures may still develop in some small regions of the optimally doped samples because of the slight local fluctuation of the doping concentration. Vortices are pinned by these interwoven domain boundaries, and therefore the stripe-like vortex patterns can appear. Because the size of these structures is small and may develop at very low temperature, for instance, even below T_c, it is not easy to detect their existence using bulk techniques. Neither the temperature-dependent resistivity nor the magnetization measurement shows any structural or magnetic transition. Nevertheless, exploiting the low-temperature local probe of structural analysis tools such as tunneling electron microscopy (TEM) and x-ray diffraction (XRD), etc., could confirm or exclude the existence of local twin domains. The origin of clustered vortex patterns may be due to the smaller size of domain structures and/or the spatial variation of T_c, which could be also introduced, for example, by nonuniform Ni-doping distribution.

Due to the local fluctuations in the doping concentration, the optimally doped sample may still have small interwoven twin boundaries in some local areas. In the overdoped pnictide superconducting sample, the absence of twin boundaries was confirmed by previous reports.[30] However the local fluctuation

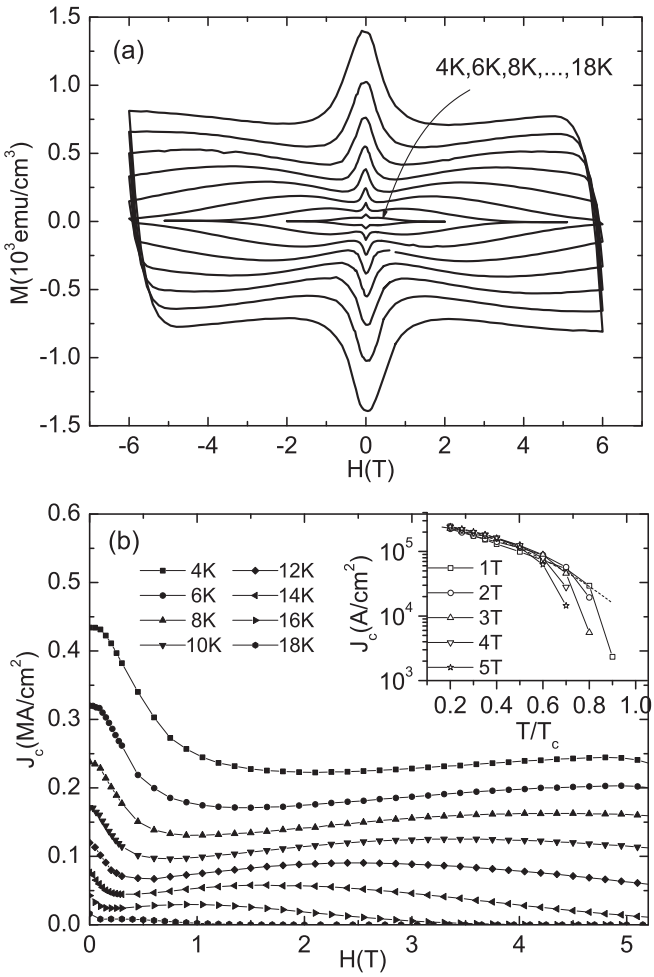

FIG. 4. Optimally doped sample $BaNi_{0.1}$: (a) Magnetic hysteresis loops M versus H at different temperatures. (b) Critical currents J_c versus H derived from the M-H loops based on the Bean critical state model. Inset of (b) shows the temperature dependence of J_c. At low temperatures, J_c(T) at different fields shows the same slow decaying rate with the increasing temperature (indicated by the dashed line).

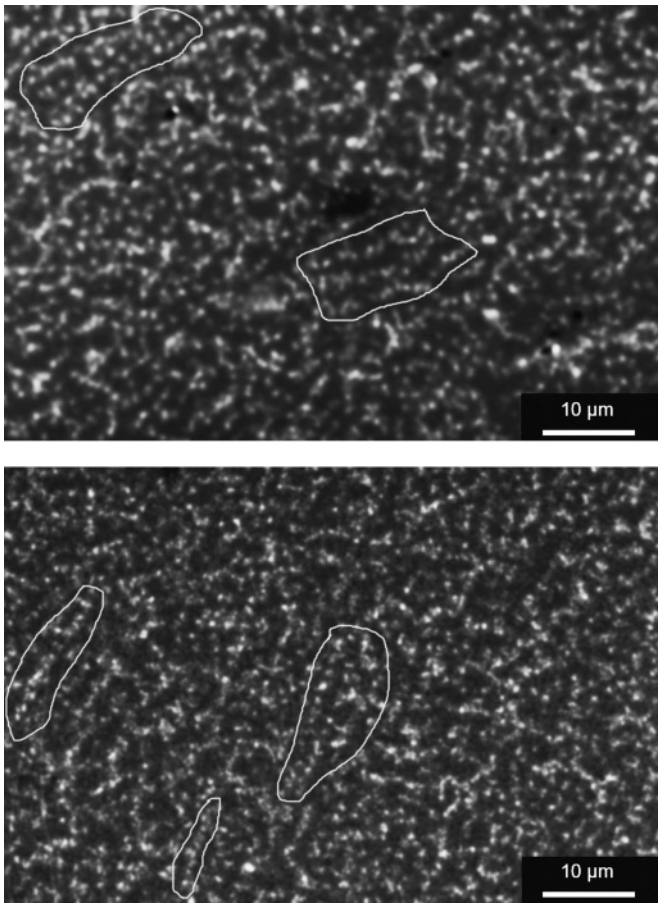

FIG. 5. Bitter decoration patterns in overdoped $BaNi_{0.16}$. Upper image: $H_a = 5$ Oe; lower image: $H_a = 10$ Oe. The stripe-like vortices are encircled by the solid lines.

of the Ni-doping level can induce the highly inhomogeneous spatial distribution of superfluid.[32] We performed EDX analysis of the local composition on both optimally doped and overdoped $BaNi_x$ single crystals. The detection in a random area ($\sim$100 μm^2) gives only 2.5% and 2.9% of the deviation in the Ni concentration from the averaged value in optimally doped and overdoped samples, respectively, which is close to other reports.[33,34] However, the spot detection carried out with the separation of a few microns, which corresponds to the spatial scale of the observed vortex inhomogeneity, shows that the content of Ni doping in some local regions presents more pronounced deviations with a maximum value up to 5% and 7%, respectively. This heavily nonuniform distribution of local doping could induce not only the highly inhomogeneous spatial distribution of superfluid but also strain in the atomic lattice, which may cause local magnetic reordering in the deformed Fe/Ni sublattice.[35]

However, within the strong pinning scenario, the fact that we observed no obvious stripe-like vortex pattern at $H_a = 1$ Oe seems to be a contradiction. The possible reason is that at $H_a = 1$ Oe, the expected separation between free vortices ($\sim$4.6 μm) is approximately equal to the separation between the stripe-like pinning centers ($\sim$5 μm) we observed at $H_a \geqslant 5$ Oe. In this case, the stripe-like vortex patterns should be difficult to resolve.

As we already pointed out in the introduction, the similar vortex distribution at low fields obtained by Bitter decoration on $BaNi_x$ and MgB_2, suggests that unconventional vortex-vortex interactions due to multiband effects could be also responsible for the inhomogeneous vortex patterns.

The large ratio between the penetration depth ($\sim$300 nm) and the coherence length ($\sim$3 nm)[13,14] indicates that the iron-pnictide superconductors could be extreme type-II superconductors. This seems to rule out the possibility of anomalous intervortex interactions due to type-1.5 behavior in iron pnictides. However, recent theoretical works[36,37] have shown the possibility of occurrence of competing long-range attractive and short-range repulsive interactions in a superconductor, which, with respect to most properties, should be an extreme type-II. According to those calculations, in a general two-band superconductor, if only one band is initially superconducting while superconductivity in the other band is induced by Josephson proximity effect from the active band, the so-called type-1.5 SC behavior will be still possible within some realistic ranges of parameters. For instance, in Ref. 33 a nonmonotonic vortex interaction has been reported

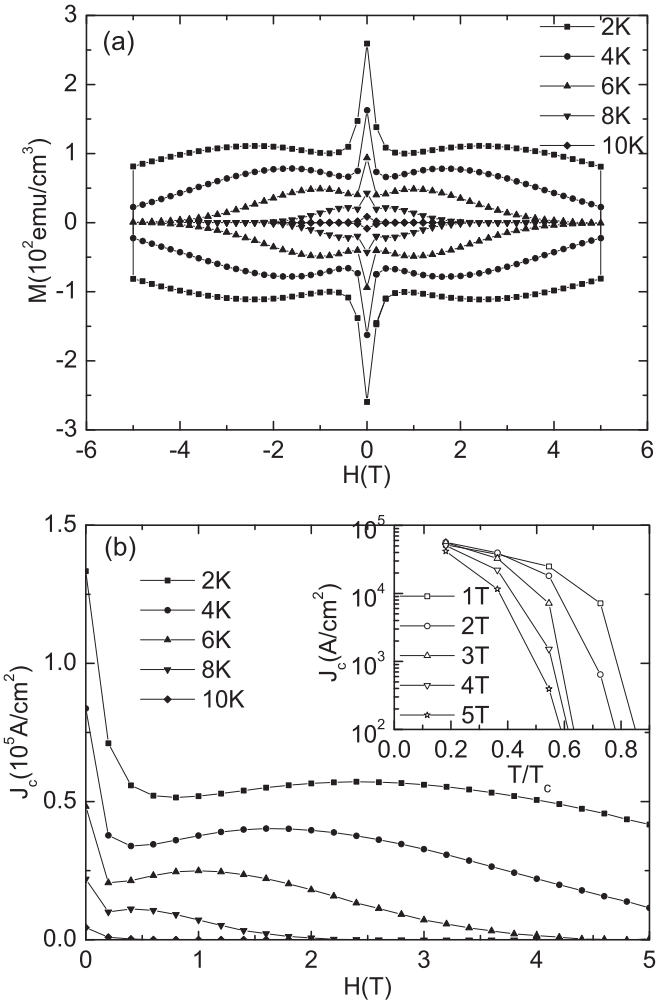

FIG. 6. Overdoped sample $BaNi_{0.16}$: (a) Magnetic hysteresis loops M versus H at different temperatures. (b) Critical currents J_c versus H derived from the M-H loops based on the Bean critical state model. Inset of (b) shows the temperature dependence of J_c. Compared with the optimally doped sample $BaNi_{0.1}$, J_c decays fast with the increasing temperature and field.

in a regime in which the dominant component has $\kappa = 8$ and an attractive interaction comes from a weak but long-range perturbation due to a coupling to a passive component. The minimum in the interaction occurs in that case at distances much larger than the London penetration depth.

One of the important factors in these calculations is that the interband Josephson coupling should be weak. However, there is no reliable, up-to-date information about the interband coupling strength in pnictide superconductors, although several arguments were given[38,39] that the interband coupling in pnictides is much stronger than that in MgB_2. On the other hand, more recent works by Carlstrom *et al.*[37,40] suggest that the fact, that Josephson coupling is strong and bands are passive, does not preclude the possibility of the type-1.5 SC regime. In this case there are just more complicated asymptotics of the tail of the order parameter. Due to the lack of sufficient experimental insight into the parameters of iron-pnictides superconductors, it is difficult to discern whether only pinning forces determine the observed inhomogeneous flux patterns in pnictides.

IV. CONCLUSIONS

We have performed Bitter decoration on multiband pnictide superconductors $BaFe_{2-x}Ni_xAs_2$ ($x = 0.1$ and $x = 0.16$) single crystals and obtained very inhomogeneous vortex patterns at low fields ($H_a \leqslant 10$ Oe). The most intriguing features are the stripe-like vortex patterns in both samples. Large-scale stripe-like vortex patterns are observed in optimally doped $BaNi_{0.1}$ single crystals, while small-size vortex stripes are observed in overdoped $BaNi_{0.16}$ single crystals. The most plausible mechanism for these stripes could be the presence of strong pinning centers, although other possibilities such as type-1.5 SC due to the multiband effect have also been discussed. Within the strong pinning scenario, for optimally doped samples, the stripe-like pinning centers could be arising from the intertwined magnetic domain boundaries induced by the local fluctuation in the Ni-doping concentration. For overdoped samples, the stripe-like pinning centers could be formed by the highly inhomogeneous superfluid distribution or the local magnetic reordering of the deformed Fe/Ni sublattice, which could be induced by the heavily local deviation in the Ni concentration. To unambiguously determine the origin of those strong pinning sources, structural analysis utilizing high resolution techniques like TEM and XRD at low temperatures should be performed. On the other hand, to elucidate the intrinsic two-band effects on the vortex behavior in the pnictide superconductors, further experiments on crystals with considerably weaker pinning are needed.

ACKNOWLEDGMENTS

This work at INPAC is supported by the FWO-Vlaanderen projects and Methusalem Funding by the Flemish government. We acknowledge helpful discussions with M. Menghini, B. Raes, and A. Silhanek.

*linjunli1981@gmail.com
†victor.Moshchalkov@fys.kuleuven.be

[1] V. G. Kogan, M. Bullock, B. Harmon, P. Miranović L. Dobrosavljević-Grujić, P. L. Gammel, and D. J. Bishop, Phys. Rev. B **55**, R8693 (1997).
[2] M. R. Eskildsen, P. L. Gammel, B. P. Barber, U. Yaron, A. P. Ramirez, D. A. Huse, D. J. Bishop, C. Bolle, C. M. Lieber, S. Oxx, S. Sridhar, N. H. Andersen, K. Mortensen, and P. C. Canfield, Phys. Rev. Lett. **78**, 1968 (1997).
[3] N. Nakai, P. Miranovic, M. Ichioka, and K. Machida, Phys. Rev. Lett. **89**, 237004 (2002).
[4] M. Yethiraj, H. A. Mook, G. D. Wignall, R. Cubitt, E. M. Forgan, S. L. Lee, D. M. Paul, and T. Armstrong, Phys. Rev. Lett. **71**, 3019 (1993).
[5] A. Grigorenko, S. Bending, T. Tamegai, S. Ooi, and M. Henini, Nature **414**, 728 (2001).
[6] J. Auer and H. Ullmaier, Phys. Rev. B **7**, 136 (1973).
[7] E. Babaev and M. Speight, Phys. Rev. B **72**, 180502(R) (2005).

[8]V. Moshchalkov, M. Menghini, T. Nishio, Q. H. Chen, A. V. Silhanek, V. H. Dao, L. F. Chibotaru, N. D. Zhigadlo, and J. Karpinski, Phys. Rev. Lett. **102**, 117001 (2009).
[9]T. Nishio, V. H. Dao, Q. H. Chen, L. F. Chibotaru, K. Kadowaki, and V. V. Moshchalkov, Phys. Rev. B **81**, 020506(R) (2010).
[10]V. H. Dao, L. F. Chibotaru, T. Nishio, and V. V. Moshchalkov, Phys. Rev. B **83**, 020503 (2011).
[11]M. R. Eskildsen, L. Y. Vinnikov, I. S. Veshchuno, T. M. Artemova, T. D. Blasius, J. M. Densmore, C. D. Dewhurst, N. Ni, A. Kreyssig, S. L. Bud'ko, P. C. Canfield, and A. I. Goldman, Physica C **469**, 529 (2009).
[12]M. R. Eskildsen, L. Y. Vinnikov, T. D. Blasius, I. S. Veshchunov, T. M. Artemova, J. M. Densmore, C. D. Dewhurst, N. Ni, A. Kreyssig, S. L. Bud'ko, P. C. Canfield, and A. I. Goldman, Phys. Rev. B **79**, 100501 (2009).
[13]Y. Yin, M. Zech, T. L. Williams, X. F. Wang, G. Wu, X. H. Chen, and J. E. Hoffman, Phys. Rev. Lett. **102**, 097002 (2009).
[14]L. Luan, O. M. Auslaender, T. M. Lippman, C. W. Hicks, B. Kalisky, J. H. Chu, J. G. Analytis, I. R. Fisher, J. R. Kirtley, and K. A. Moler, Phys. Rev. B **81**, 100501 (2010).
[15]L. J. Li, Y. K. Luo, Q. B. Wang, H. Chen, Z. Ren, Q. Tao, Y. K. Li, X. Lin, M. He, Z. W. Zhu, G. H. Cao, and Z. A. Xu, New J. Phys. **11**, 025008 (2009).
[16]L. Ding, J. K. Dong, S. Y. Zhou, T. Y. Guan, X. Qiu, C. Zhang, L. J. Li, X. Lin, G. H. Cao, Z. A. Xu, and S. Y. Li, New J. Phys. **11**, 093018 (2009).
[17]S. Chi, A. Schneidewind, J. Zhao, L. W. Harriger, L. Li, Y. Luo, G. Cao, Z. Xu, M. Loewenhaupt, J. Hu, and P. Dai, Phys. Rev. Lett. **102**, 107006 (2009).
[18]S. Li, Y. Chen, J. W. Lynn, L. Li, Y. Luo, G. Cao, Z. Xu, and P. Dai, Phys. Rev. B **79**, 174527 (2009).
[19]The actual composition are BaNi0.096 $\pm$ 0.003 and BaNi0.161 $\pm$ 0.004. For the convenience, we will use the nominal content in the rest part of the text.
[20]B. Shen, P. Cheng, Z. S. Wang, L. Fang, C. Ren, L. Shan, and H. H. Wen, Phys. Rev. B **81**, 014503 (2010).
[21]S. Salem-Sugui, L. Ghivelder, A. D. Alvarenga, L. F. Cohen, K. A. Yates, K. Morrison, J. L. Pimentel, H. Luo, Z. Wang, and H.-H. Wen, Phys. Rev. B **82**, 054513 (2010).
[22]R. Prozorov, M. A. Tanatar, E. C. Blomberg, P. Prommapan, R. T. Gordon, N. Ni, S. L. Bud'ko, and P. C. Canfield, Physica C: Superconductivity **469**, 667 (2009).
[23]C. P. Bean, Rev. Mod. Phys. **36**, 31 (1964).
[24]C. U. Jung, J. Y. Kim, P. Chowdhury, K. H. P. Kim, S. I. Lee, D. S. Koh, N. Tamura, W. A. Caldwell, and J. R. Patel, Phys. Rev. B **66**, 184519 (2002).
[25]G. J. McIntyre, A. Renault, and G. Collin, Phys. Rev. B **37**, 5148 (1988).
[26]G. Blatter, M. V. Feigel'man, V. B. Geshkenbein, A. I. Larkin, and V. M. Vinokur, Rev. Mod. Phys. **66**, 1125 (1994).
[27]L. Y. Vinnikov, J. Anderegg, S. L. Bud'ko, P. C. Canfield, and V. G. Kogan, Phys. Rev. B **71**, 224513 (2005).
[28]H. Bluhm, S. E. Sebastian, J. W. Guikema, I. R. Fisher, and K. A. Moler, Phys. Rev. B **73**, 014514 (2006).
[29]M. A. Tanatar, A. Kreyssig, S. Nandi, N. Ni, S. L. Bud'ko, P. C. Canfield, A. I. Goldman, and R. Prozorov, Phys. Rev. B **79**, 180508 (2009).
[30]B. Kalisky, J. R. Kirtley, J. G. Analytis, J. H. Chu, A. Vailionis, I. R. Fisher, and K. A. Moler, Phys. Rev. B **81**, 184513 (2010).
[31]R. Prozorov, M. A. Tanatar, N. Ni, A. Kreyssig, S. Nandi, S. L. Bud'ko, A. I. Goldman, and P. C. Canfield, Phys. Rev. B **80**, 174517 (2009).
[32]T. H. Kim, R. Jin, L. R. Walker, J. Y. Howe, M. H. Pan, J. F. Wendelken, J. R. Thompson, A. S. Sefat, M. A. McGuire, B. C. Sales, D. Mandrus, and A. P. Li, Phys. Rev. B **80**, 214518 (2009).
[33]P. C. Canfield, S. L. Bud'ko, N. Ni, J. Q. Yan, and A. Kracher, Phys. Rev. B **80**, 060501 (2009).
[34]J. H. Chu, J. G. Analytis, C. Kucharczyk, and I. R. Fisher, Phys. Rev. B **79**, 014506 (2009).
[35]T. Yildirim, Phys. Rev. Lett. **101**, 057010 (2008).
[36]E. Babaev, J. Carlstrom, and M. Speight, Phys. Rev. Lett. **105**, 067003 (2010).
[37]J. Carlstrom, E. Babaev, and M. Speight, Phys. Rev. B **83**, 174509 (2011).
[38]O. V. Dolgov, I. I. Mazin, D. Parker, and A. A. Golubov, Phys. Rev. B **79**, 060502 (2009).
[39]L. Fanfarillo, L. Benfatto, S. Caprara, C. Castellani, and M. Grilli, Phys. Rev. B **79**, 172508 (2009).
[40]J. Carlstrom, J. Garaud, and E. Babaev, e-print arXiv:1101.4599 (2011).